Optics Letters

$Nd:YVO_4$ high-power master oscillator power amplifier laser system for second-generation gravitational wave detectors

Fabian Thies,[1,*] Nina Bode,[1] Patrick Oppermann,[1] Maik Frede,[2] Bastian Schulz,[2] and Benno Willke[1]

[1]Max-Planck-Institut für Gravitationsphysik (Albert-Einstein-Institut) and Leibniz Universität Hannover, Callinstr. 38, 30167 Hannover, Germany
[2]neoLASE GmbH, Hollerithallee 17, 30419 Hannover, Germany
*Corresponding author: fabian.thies@aei.mpg.de

Received 4 December 2018; accepted 17 December 2018; posted 2 January 2019 (Doc. ID 354549); published 31 January 2019

Ultrastable high-power laser systems are essential components of the long baseline interferometers that detected the first gravitational waves from merging black holes and neutron stars. One way to further increase the sensitivity of current generation gravitational wave detectors (GWDs) is to increase the laser power injected into the interferometers. In this Letter, we describe and characterize a 72 W and a 114 W linearly polarized, single-frequency laser system at a wavelength of 1064 nm, each based on single-pass $Nd:YVO_4$ power amplifiers. Both systems have low power and frequency noise and very high spatial purity with less than 10.7% and 2.9% higher order mode content, respectively. We demonstrate the simple integration of these amplifiers into the laser stabilization environment of operating GWDs and show stable low-noise operation of one of the amplifier systems in such an environment for more than 45 days.

https://doi.org/10.1364/OL.44.000719

In 2015, two Advanced Laser Interferometer Gravitational-Wave Observatory (LIGO) detectors measured the first gravitational wave from two merging black holes, and later in 2017, a network extended by the Advanced Virgo detector was able to detect gravitational waves from merging neutron stars [1–4]. These discoveries opened a new observation window to the universe and are a milestone in multimessenger astronomy [5]. One of the key components of the long baseline interferometers used for these detections are high-power (HP) prestabilized laser systems (PSLs) with high spatial mode purity and high reliability. To increase their sensitivity and the corresponding gravitational wave detection rate, the Advanced LIGO and the Advanced Virgo detectors have upgraded their laser systems. Both upgrades are based on slightly different four-stage single-pass $Nd:YVO_4$ amplifiers seeded by the existing master oscillator power amplifier (MOPA) lasers.

In this Letter, we characterize both amplifier types by seeding them with a MOPA laser of an Advanced LIGO laser system [6] and analyze the resulting laser beam with a diagnostic breadboard (DBB) [7]. Furthermore, we demonstrate that the amplifiers are compatible with gravitational wave detector (GWD) stabilization concepts and show long-term stable operation of a full prestabilized GWD laser system based on one of these amplifiers.

We used a copy of the Advanced LIGO PSL (aLIGO PSL) [6], called the reference system, as the environment to test two slightly different solid-state $Nd:YVO_4$ amplifiers. The first amplifier was a neoVAN-4S and the second a neoVAN-4S-HP, both manufactured by neoLASE.

The neoVAN-4S and neoVAN-4S-HP amplifiers consist of four $Nd:YVO_4$ crystals. Each crystal is pumped with a fiber-coupled laser diode. The crystals of the neoVAN-4S amplifier are optimized for the used pump wavelength of 808 nm, while the crystals of the HP version are optimized for the pump wavelength of 878 nm. For the neoVAN-4S, a pump power of 30 W to 35 W of the maximal available 45 W is used with standard current drivers. The neoVAN-4S-HP amplifier uses 50 W to 55 W of the maximal available 65 W per crystal with external low-noise current supplies. Both amplifier types are seeded with linear *s*-polarized laser light at 1064 nm wavelength and in the fundamental Gaussian mode. Their laser heads, as well as the pump laser diodes, are water cooled.

Our MOPA laser of the Advanced LIGO laser system [8,9] is used as seed laser for the investigations of the neoVAN amplifiers, and the DBB [7] of this system is used to characterize the amplified laser beams (see Fig. 1).

The DBB performs a fully automated characterization of the lasers by measuring the higher order mode content, the relative power noise, the frequency noise, and pointing noise of the laser beam relative to an acoustically shielded Fabry–Perot ring cavity. The length of the cavity is stabilized to the laser frequency, and the beam alignment is stabilized to the fundamental eigenmode of the cavity. We used the error and control signal of the feedback control loops to calculate the amplitude spectral density of the noises in a frequency range of 1 Hz to 10 kHz, which is the most relevant range for current GWDs. In addition, the measurement of the higher order spatial mode content is performed by multiple-length scans over the free spectral range of the resonator.

The neoVAN-4S amplifier was tested with a seed power of 28 W. For this test, the higher order mode content of the seed laser was 7.1%. This results in an amplified output power of

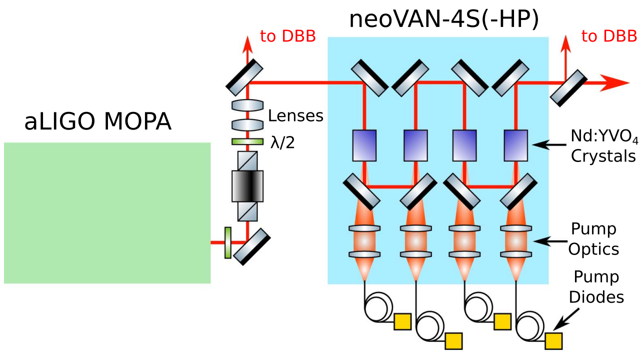

Fig. 1. Schematic setup of the light power amplifier system with our aLIGO MOPA laser as the seed source. A fraction of the light from the aLIGO MOPA laser and from the neoVAN amplifier is used for characterization with the diagnostic breadboard (DBB).

72 W in linear polarization with a higher order mode content of 10.7%, measured with the DBB. This neoVAN amplifier was sent to and installed at one of the Advanced LIGO detectors after characterization.

Furthermore, two neoVAN-4S-HP amplifiers were operated and tested with output powers of 111 and 114 W. The first one is now in use at the Virgo GWD, and the second was characterized in detail for more than 45 days in our lab. In this Letter, we show performance data of the second amplifier.

For the neoVAN-4S-HP test, we reduced the power of the seed beam to 27 W, which reduced its higher order mode content to 2.7%. With this seed beam, the output beam of the neoVAN-4S-HP amplifier was analyzed to have only 2.9% higher order mode content and an optical power of 114 W.

In Fig. 2, the output power of the neoVAN-4S-HP amplifier is shown as a function of the seed power. The extracted power computed as the power added by the amplifier to the seed power is higher than 80 W for seed powers above 5 W. For this measurement, the seed power was attenuated by a half-wave plate and polarizing beam splitter combination.

To purify the spatial beam profile and reduce beam pointing, the beam of GWD lasers is filtered by premode cleaner cavities (PMCs) [6]. We coupled the amplified beam to an aLIGO PMC and plotted the transmitted power as an additional data set in Fig. 2.

For different seed powers, realignment of neither the amplifier nor the resonator downstream the amplifier was necessary. A complete set of DBB beam characterization measurements was performed for different seed powers (1.7 W, 12 W, 27 W).

In this Letter, we present the results for the neoVAN-4S-HP seeded with 27 W in blue and the neoVAN-4S seeded with 28 W in red. The measurements of the corresponding seed laser beams are plotted in dotted lines.

The relative power noises are shown in Fig. 3. At low frequencies, the transfer function from relative seed power fluctuations to the output power of largely saturated amplifiers is much smaller than the transfer of relative pump power noise [10]. Hence, the power noise of the neoVAN amplifiers is most likely dominated by fluctuations in the power of the pump laser diodes and correspondingly by fluctuations of their current source. For the investigations of the neoVAN-4S-HP, we replaced the standard neoLASE power supplies (used for the neoVAN-4S measurement) with low-noise Delta SM800 power supplies. Due to unavailable data on the pump light fluctuations and on the saturation level of the different amplifier stages, no quantitative pump-light noise projection was possible. Nevertheless, the measurements clearly indicate the benefit of a quitter power supply. Figure 4 shows a high-frequency noise measurement of the relative power noise of the neoVAN-4S-HP.

The frequency noises of the free-running amplifiers are characterized using the DBB and are shown in Fig. 5 in comparison to the free-running noises of the seed laser. In the full measured Fourier frequency band, the frequency noise of the free-running amplifiers is similar to the noise of our aLIGO MOPA laser, which is close to the typical nonplanar ring oscillator (NPRO) laser noise.

The beam pointing was measured with the automatic alignment system of the DBB. We use the quantity $\epsilon(t) = \delta x(t)/w_0 + i\delta\alpha(t)/\Theta_D$ with the transverse shift of the beam $\delta x(t)$ normalized by the beam waist radius w_0 and the tilt $\delta\alpha(t)$ normalized to the half-divergent angle of the beam Θ_D to quantify the beam pointing. The pointing noise measurements were taken at +45° and –45% Gouy phase position,

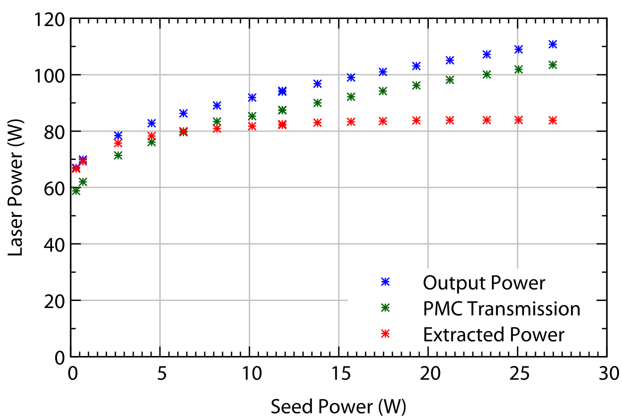

Fig. 2. Output power of the neoVAN-4S-HP amplifier and the power transmitted by a premode cleaner (PMC) filter cavity are shown as a function of the seed power. The difference between the power after and before the amplifier (extracted power) is nearly constant for seed powers above 5 W.

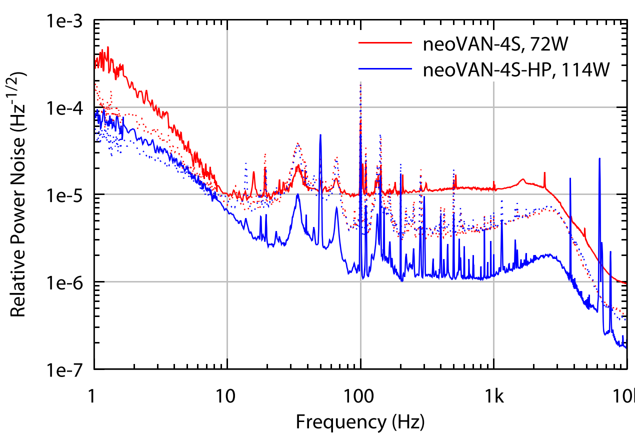

Fig. 3. Amplitude spectral density of the relative power noise of the 72 W and 114 W laser beams (solid lines) and the corresponding seed laser beams (dotted lines).

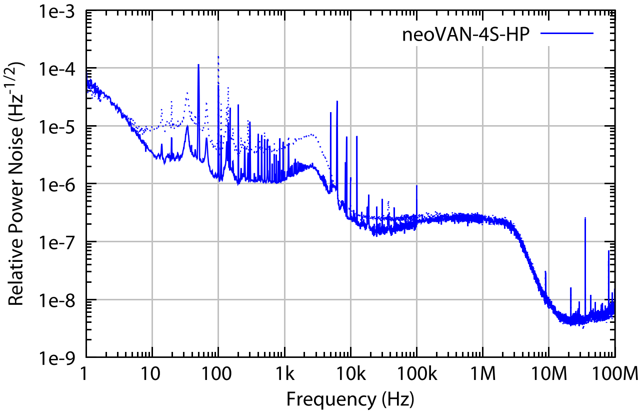

Fig. 4. Amplitude spectral density of the relative power noise of the 114 W laser beam (solid line) and of the corresponding seed laser beam (dotted line) for Fourier frequencies up to 100 MHz. Beyond 20 MHz, the measured noise is close to the shot noise of the detected photocurrent. The peak at 35 MHz corresponds to modulation sidebands used for the feedback control loops.

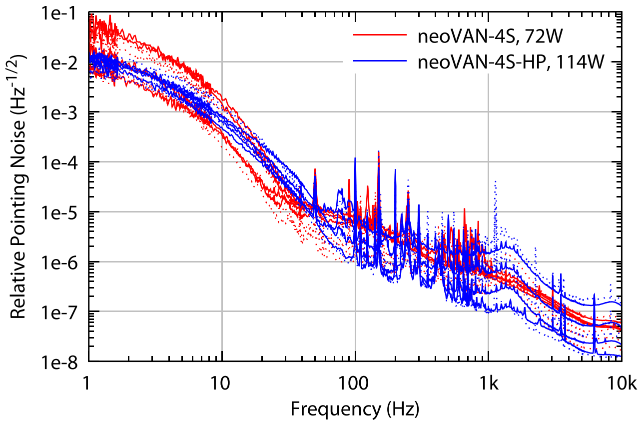

Fig. 6. Pointing noise in all four alignments degrees of freedom is shown as an amplitude spectral density over the Fourier frequency. The pointing noise of the amplifiers (solid lines) is dominated by the low pointing noise of the seed laser (dotted lines).

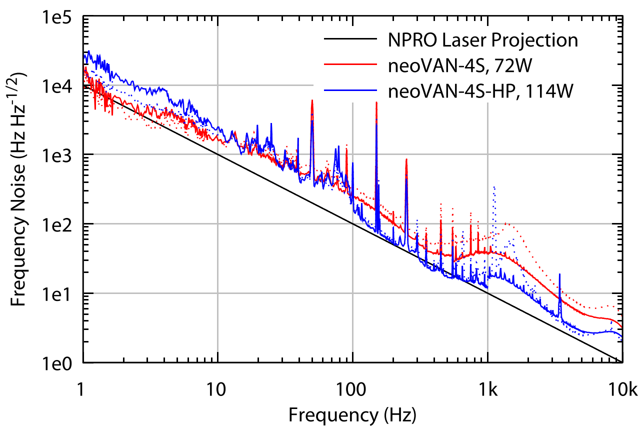

Fig. 5. Using the diagnostic breadboard, measurements of the frequency noise were performed and are shown as an amplitude spectral density over the Fourier frequency. The frequency noises of the free-running amplifiers (solid lines) are mostly dominated by the frequency noises of the seed laser (dotted lines) and close to the typical frequency noise of NPRO lasers.

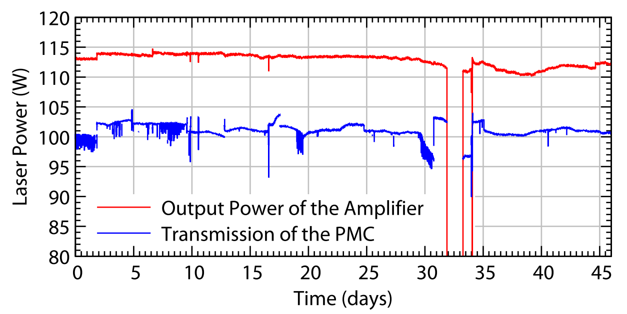

Fig. 7. Long-term measurement of the output power of the amplifier and in transmission of the premode cleaner cavity (PMC) shows the stability of the system over time. The PMC transmission shows dips due to automatic relocking of the laser system. Between days 34 and 37, the laser system was switched off and on again and recovered operation at the same performance as before without any realignment of the amplifier.

corresponding to the readout of $\epsilon(t)$ projected under these angles. By measuring the pointing in the horizontal and vertical direction, in total, four noise spectra are recorded [7]. The pointing noise of the amplified beams is close to the low noise level of the seed laser (see Fig. 6). The low pointing noise of the neoVAN-4S-HP was analyzed in daily measurements over 45 days and did not show significant variations.

The integration of a neoVAN amplifier into the aLIGO PSL [6] requires only a simple modification of the beam path. This modification routes our aLIGO MOPA into the neoVAN amplifier and its output beam into the original HP beam path towards the aLIGO PMC. As this PMC serves as the spatial interface towards the main interferometer and the power and frequency stabilization subsystems, a matching of the neoVAN beam to the PMC simultaneously provides a good alignment to these systems. Such a modification was performed at the aLIGO PSL reference system in our lab. All PSL feedback control loops could be engaged without major modification and achieved the stability requirements of aLIGO.

The output power of the neoVAN-4S-HP amplifier and the transmitted power through the PMC are shown in Fig. 7 for an operation time of more than 45 days. The average transmitted power through the PMC is 95% of the incident power. This is consistent with the results of the mode scans performed with the DBB. Due to temperature fluctuations in the laboratory, the PMC had to be realigned after several days to stay at the HP transmission level.

The frequency stabilization control loop of the laser system to a reference cavity is not affected by the integration of the amplifier and thereby reached its design stability and unity gain frequency. The power stabilization of the system was performed using a HP acousto-optic modulator (AOM) to split off power into the first diffraction order. Two photodiodes detecting a

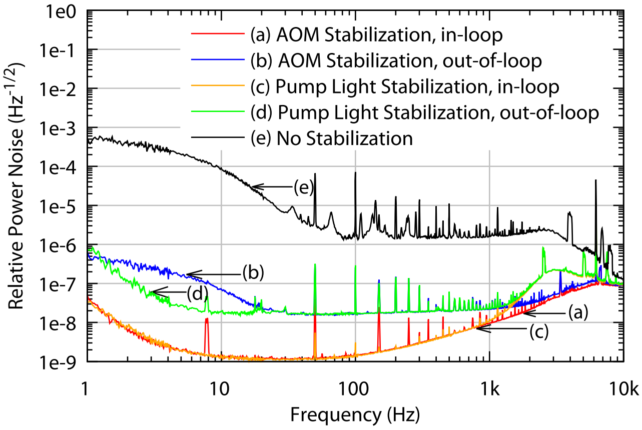

Fig. 8. Two separated photodiodes of the same kind were used to perform a measurement of the relative power noise. This is shown as an amplitude spectral density over the Fourier frequency. One photodiode is used as an out-of-loop detector, while the other one is used for the active feedback stabilization. The power stabilization of the system was performed with two different power actuators (see text).

photo current of 2.8 mA are used as the in-loop and out-of-loop sensor for the active feedback stabilization of the laser power in transmission of the PMC. This stabilization reaches the required stability shown in Fig. 8. In a frequency range from 20 Hz to 2 kHz, the achieved stability is limited by the shot noise of the sensors.

A fast power control of the pump light of the last laser crystal in the neoVAN-4S-HP amplifier makes a power stabilization without an AOM in the beam path possible. Such an AOM adds additional loss and can produce stray light, a thermal lens, or spatial beam distortion.

An in-house-developed controllable bypass resistor is used to control the current through one laser diode of the neoVAN-4S-HP amplifier and thereby its output power. This circuit is a high current version of the actuator used in Ref. [11] with a current modulation bandwidth of 800 kHz, achieved with a feedback controlled MOSFET transistor and low inductance resistors. We were able to operate this power stabilization with a high noise suppression. The used feedback stabilization had a unity gain frequency of 45 kHz. In Fig. 8, the resulting noise is compared to the stabilization with the AOM.

As the coupling of power noise to the GWD output is most significant at low frequencies, the noise bump around 3 kHz is less significant than the improved stability below 13 Hz.

In this Letter, we characterize two types of HP solid-state amplifiers and show that those are useful extensions of the laser systems of currently operating GWDs. We show that such amplifiers are easy to integrate into the aLIGO PSL and can generate up to 114 W power in a low-noise laser beam with more than 97% in the fundamental spatial mode. We present a power stabilization scheme with feedback to the pump diode current and show stable long-term operation of one of the amplifiers as an integral part of a prestabilized GWD laser system. In addition to their use in currently operating GWDs, these amplifiers are good candidates for a setup to generate even higher power levels by means of coherent beam combination [12].

Funding. German Volkswagen Foundation.

REFERENCES

1. J. Aasi, B. P. Abbott, R. Abbott, and T. Abbott, and LIGO Scientific Collaboration, Classical Quantum Gravity **32**, 074001 (2015).
2. F. Acernese, P. Amico, N. Arnaud, and D. Babusci, and Virgo Collaboration, Classical Quantum Gravity **32**, 024001 (2014).
3. B. P. Abbott, S. Jawahar, N. A. Lockerbie, and K. V. Tokmakov, LIGO Scientific Collaboration, and Virgo Collaboration, Phys. Rev. Lett. **116**, 061102 (2016).
4. B. P. Abbott, S. Jawahar, N. A. Lockerbie, and K. V. Tokmakov, LIGO Scientific Collaboration, and Virgo Collaboration, Phys. Rev. Lett. **119**, 141101 (2017).
5. B. P. Abbott, S. Jawahar, N. A. Lockerbie, and K. V. Tokmakov, LIGO Scientific Collaboration, and Virgo Collaboration, Astrophys. J. **848**, L12 (2017).
6. P. Kwee, C. Bogan, K. Danzmann, M. Frede, H. Kim, P. King, J. Pöld, O. Puncken, R. L. Savage, F. Seifert, P. Wessels, L. Winkelmann, and B. Willke, Opt. Express **20**, 10617 (2012).
7. P. Kwee and B. Willke, Appl. Opt. **47**, 6022 (2008).
8. L. Winkelmann, O. Puncken, R. Kluzik, C. Veltkamp, P. Kwee, J. Poeld, C. Bogan, B. Willke, M. Frede, J. Neumann, P. Wessels, and D. Kracht, Appl. Phys. B **102**, 529 (2011).
9. M. Frede, B. Schulz, R. Wilhelm, P. Kwee, F. Seifert, B. Willke, and D. Kracht, Opt. Express **15**, 459 (2007).
10. M. Tröbs, P. Weßels, and C. Fallnich, Opt. Express **13**, 2224 (2005).
11. R. S. Abbott and P. J. King, Rev. Sci. Instrum. **72**, 1346 (2001).
12. H. Tünnermann, J. H. Pöld, J. Neumann, D. Kracht, B. Willke, and P. Weßels, Opt. Express **19**, 19600 (2011).